Bottom-Up Approaches for Precisely Nanostructuring Hybrid Organic/Inorganic Multi-Component Composites for Organic Photovoltaics

Lingyao Meng[1], Hongyou Fan[2], J. Matthew D. Lane[2], Yang Qin[1]

[1]Department of Chemistry and Chemical Biology, University of New Mexico, Albuquerque, New Mexico, United States.

[2]Sandia National Laboratories, Albuquerque, New Mexico, United States.

Abstract:

Achieving control over the morphology of conjugated polymer (CP) blends at nanoscale is crucial for enhancing their performances in diverse organic optoelectronic devices, including thin film transistors, photovoltaics, and light emitting diodes. However, the complex CP chemical structures and intramolecular interactions often make such control difficult to implement. We demonstrate here that cooperative combination of non-covalent interactions, including hydrogen bonding, coordination interactions, and π-π interactions, etc., can be used to effectively define the morphology of CP blend films, in particular being able to achieve accurate spatial arrangement of nanoparticles within CP nanostructures. Through UV-vis absorption spectroscopy and transmission electron microscopy, we show strong attachment of fullerene molecules, CdSe quantum dots, and iron oxide nanoparticles, onto well-defined CP nanofibers. The resulting core/shell hybrid nanofibers exhibit well-defined donor/acceptor interface when employed in photovoltaic devices, which also contributes to enhanced charge separation and transport. These findings provide a facile new methodology of improving CP/nanoparticle interfacial properties and controlling blend morphology. The generality of this methodology demonstrated in current studies points to a new way of designing hybrid materials based on organic polymers and inorganic nanoparticles towards applications in modern electronic devices.

INTRODUCTION:

In recent years, conjugated polymers (CPs) have been intensively studied for applications in flexible electronic devices, including organic field effect transistors (OFETs) [1-3], organic photovoltaics (OPVs), [4-8] and organic light emitting diodes (OLEDs) [9, 10], thanks to their unique properties when compared with the inorganic counterparts, including highly tunable optoelectronic properties, solution processability, and mechanical flexibility. In particular, CP based OPVs have been considered as a promising alternative energy technology for the lightweight, flexibility, low-cost, and amenability to industrial high-throughput roll-to-roll processing [11, 12]. It has been well understood that in OPV devices, excitons generated in CPs upon light absorption can only be effectively harvested through donor/acceptor heterojunction morphology by blending with another material with larger electron affinity, *i.e.*, electron acceptor [13]. So far, a variety of materials, including electron deficient CPs [14-16], fullerene derivatives [5, 17], small organic molecules [18], inorganic semiconductor nanoparticles [19, 20], and metal oxides [21, 22], have all been extensively studied as electron acceptors in OPV devices in combination with CPs. Because of the limited exciton diffusion lengths of CPs, the overall performance of OPV devices, which is a synergistic outcome from carrier generation, separation, and transport, is heavily dependent on the morphologies and interfaces between the electron donor and acceptor materials. It has been demonstrated that the state-of-the-art blend morphologies in OPVs are the so-called bulk heterojuntion (BHJ) that is characterized by percolating networks of donor and acceptor domains having sizes of ca. 10 nm.[23-25] However, BHJ is mostly optimized by trial-and-error approaches, such as thermal/solvent annealing [26, 27] and processing with solvent additives [28], which are system dependent and lead to batch-to-batch variations. The phase separation at nanometer scales between the donor and acceptor components is typically trapped at a thermodynamically meta-stable state, leading to instability issues for long-term applications.

Among the many CPs studied in OPV devices, regio-regular poly(3-hexylthiophene) (P3HT) has been one of the most studied and one of the few CPs that can crystalize into well-defined nanostructures. Under certain conditions, P3HT can form uniform nanofibers (NFs) having widths of ca. 15–20 nm and lengths up to a few μm, which have shown improved charge mobility [29, 30] and exciton diffusion lengths [31-35]. OPV devices by blending P3HT NFs with fullerene derivatives have been shown to outperform devices employing conventional BHJ [36-39]. However, simple mixing of P3HT NFs with another electron acceptor material often results in uncontrolled macrophase separations due to the frequently encountered chemical incompatibility, while the resulting morphology still suffers from long-term thermal instability.

In order to stabilize BHJ morphologies at the right length scales while maintaining the favourable electronic properties in P3HT crystallites, one commonly applied strategy is the utilization of P3HT-containing block copolymers (BCPs) having electron acceptor moieties selectively attached to one functionalized block [40-44]. Examples reported so far have mostly been focused on covalent attachment of fullerene units [45-48]. However, in these examples, the fullerene loading percentages are generally low caused by the strong aggregation tendency of fullerenes that result in poor solubility of resulting polymers at high fullerene loadings. An alternative approach that can

potentially alleviate the above problems is to attach fullerene acceptors, as well as other nanoparticles, non-covalently. Existing examples have demonstrated attachment of fullerene derivatives to P3HT based BCPs through π-π [49, 50] and simple hydrogen bonding [51, 52] interactions. These interactions are however relatively weak and the resulting blend films did not show significantly improved thermal stability. Furthermore, few studies have been carried out on the formation of BHJs from self-assembly of conjugated BCPs with inorganic nanoparticles. Su *et al.* [53], Stefan *et al.* [54] and Chen *et al.* [55] all reported the incorporation of inorganic nanoparticles through covalent attachment onto P3HT-containing BCPs, which suffer similar drawbacks as those fullerene systems discussed above.

Herein, we present a general approach for the preparation of stable and well-ordered CP/nanoparticle blends through strong cooperation of several non-covalent interactions including BCP crystallization, nanoparticle aggregation, π-π interactions, complementary hydrogen bonding and coordination interactions. BCPs with P3HT backbone and isoorotic acid or pyridine as side chain functional groups were designed and synthesized. Mixed solvent approach was used to achieve the crystallization of BCPs into core/shell NFs. Organic and inorganic nanoparticles, including fullerene derivatives PCBM ([6,6]-phenyl-C61-butyric acid methyl ester), CdSe quantum dots (QDs), and iron oxide nanoparticles (IONPs) were then attached onto BCP NFs through hydrogen bonding, π-π interactions, and/or coordination interactions to form well-controlled hybrid polymer/nanoparticle core/shell composite NFs. These composite NFs are then applied in OPVs and devices employing P3HT/fullerene composite nanofibers out-perform those using P3HT homopolymers under optimized conditions..

EXPERIMENTAL DETAILS:

Synthetic procedures

All reagents and solvents were purchased from Sigma-Aldrich, TCI America, or Alfa Aesar, and used as received. [6,6]-Phenyl-C61-butyric acid methyl ester (PCBM) was purchased from American Dye Source. Tetrahydrofuran (THF) was dried by distillation from sodium-benzophenone before use.

Poly(3-hexylthiophene) (P3HT). A flame dried 100 mL round bottom flask equipped with stopcocks, septa and magnetic stir bar was charged with M1 (0.5 g, 1.34 mmol) and LiCl (0.032 g, 0.75 mmol), and 24 mL anhydrous THF was added into the flask by syringe at room temperature. The solution was then cooled to 0 °C, and 2 M solution of i-PrMgCl in THF (0.67 mL, 1.34 mL) was added. After stirring for 30 min, the solution was heated to 35 °C, and Ni(dppp)Cl$_2$ catalyst (7.5 mg, 0.0134 mmol) suspended in 2.3 mL THF was injected and stirred for 10 min. The reaction mixture was then quenched with methanol. The resulting polymer was purified by Soxhlet extractions using methanol, acetone, hexanes, THF and chloroform. The final product was recovered by precipitation of the chloroformr solution into methanol, and vacuum dried at 50 °C for 24 h (black powder, 46 % yield). ^{1}H NMR (300.13 MHz, CDCl$_3$): δ (ppm) = 6.98 (Th-*H*), 2.80(Th-C*H$_2$*), 1.71 (Th-CH$_2$C*H$_2$*), 1.40 (Th-CH$_2$CH$_2$[C*H$_2$*]$_3$CH$_3$), 0.94 (Th-CH$_2$CH$_2$[CH$_2$]$_3$C*H$_3$*). SEC (CHCl$_3$, 1 mL/min): Mn = 19.5 kDa, Mw = 23.4 kDa, PDI = 1.2.

BCP1. In a 100 mL flame dried round bottom flask, M1 (1 g, 2.69 mmol) and LiCl (0.576 g , 1.34 mmol) were pumped overnight to remove any water and oxygen. 50

mL dry THF was then added into the flask and the solution was cooled to 0 °C. Next, 1.98 mL i-PrMgCl solution (2 M in THF) was injected into the flask via syringe, and the mixture was stirred for 30 min (solution 1). In another 25 mL flame dried round bottom flask, M2 (0.134 g, 0.268 mmol) and LiCl (0.058 g, 0.134 mmol) were added, and the flask was degassed under vacuum overnight. 5 mL anhydrous THF was added to the reaction mixture and the solution was stirred for 30 min at 0 °C. Solution 1 was then heated up to 35 °C, and Ni(dppp)Cl$_2$ catalyst (7.6 mg in 2.3 mL THF) was added, and the solution was stirred for 30 min. 0.3 mL aliquot was then taken and quenched into excess EtMgBr. SEC (CHCl$_3$, 1 mL/min): Mn = 37.9 kDa, Mw = 42.7 kDa, PDI = 1.1. Solution 2 was then transferred into solution 1 via cannula transfer. After 45 min, the reaction was quenched by adding 2 mL EtMgCl (2 M in THF). The polymer was precipitated into methanol, and purified by Soxhlet extractions with methanol, acetone, hexanes, THF and chloroform. The final product was then precipitated into methanol, collected by filtration, dried overnight as a black powder (56% yield). ^{1}H NMR (300.13 MHz, CDCl$_3$): δ (ppm) = 6.98 (Th-*H*), 3.65 (-O-C*H$_2$*CH$_2$-), 2.80 (Th-C*H$_2$*), 1.71-0.83 (alkyl-*H*'s). SEC (CHCl$_3$, 1 mL/min): Mn = 46.6 kDa, Mw = 52.7 kDa, PDI = 1.1.

BCP2. In a dry, 50 mL round bottom flask, 150 mg BCP1 was dissolved in 120 mL dry THF and stirred under nitrogen at 60 °C for 30 min. Afterwards, tetrabutylammonium fluoride (TBAF) solution (1.1 mL, 1M in THF) was added dropwise via syringe and the solution was stirred at 60 °C for 9 h. The polymer was recovered by precipitation into methanol and then dried overnight under vacuum (black powder, 86% yield). ^{1}H NMR (300.13 MHz, CDCl$_3$): δ (ppm) = 6.98 (Th-*H*), 3.66 (C*H$_2$*OH), 2.80 (Th-C*H$_2$*), 1.71-0.83 (alkyl-*H*'s). SEC (CHCl$_3$, 1 mL/min): Mn = 32.9 kDa, Mw = 37.8 kDa, PDI = 1.2.

BCP3 [56-58]**.** A 25 mL round bottom flask equipped with a condenser, a septa and a nitrogen inlet was filled with 1-n-hexylisoorotic acid (1.02 mmol) and thionyl chloride (2 mL). The solution was heated under refluxed for 8 h to synthesize the acid chloride. After the reaction, excess SOCl$_2$ was removed by vacuum. In another 250 mL Schlenk flask, 200 mg BCP2 and 30 mL CHCl$_3$ was mixed and kept stirring at 60 °C for 30 min. Subsequently, 0.3 mL triethylamine was added into the reaction mixture. The acid chloride dissolved in 15 mL CHCl$_3$ was then transferred into the polymer solution via cannula transfer. After 8 h, the solution was concentrated and the product was recovered by precipitation into methanol, and then purified by Soxhlet extractions with methanol, acetone, and chloroform. The final polymer (black solid) was then collected by precipitation into methanol and dried under vacuum overnight (78% yield). ^{1}H NMR (300.13 MHz, CDCl$_3$): δ (ppm) = 6.98 (Th-*H*), 4.26 (NC*H$_2$*-), 3.77 (-COOC*H$_2$*-), 2.80-0.92 (hexyl-*H*'s and methylene-*H*'s). SEC (CHCl$_3$, 1 mL/min) at 35 °C: Mn = 27.2 kDa, Mw = 43.5 kDa, PDI = 1.6.

BCP4 [59]**.** In a 100 mL Schlenk flask, 65.1 mg BCP2, 23 mg 4-dimethylaminopyridine (0.19 mmol) and 15 mL anhydrous chlorobenzene were mixed and heated to 90 °C and stirred for 30 min. Nicotinoyl chloride hydrochloride complex (17.1 mg, 0.09 mmol) was then added as a solid, and the solution was stirred at 90 °C for 8 h. Finally, the crude polymer product was precipitated into methanol, and then purified by sequential Soxhlet extractions with methanol, acetone, hexanes, THF and chloroform. The final product was isolated from the chloroform extraction, precipitated into methanol, and dried at 50 °C under vacuum for 24 h (black powder, 91% yield). ^{1}H NMR (300.13 MHz, CDCl$_3$): δ (ppm) = 9.27, 8.75, 8.28 (Py-*H*'s), 6.98 (Th-*H*), 4.37 (-C*H$_2$*OOC-), 2.80 (Th-C*H$_2$*), 1.71-0.83 (alkyl-*H*'s). SEC (CHCl$_3$, 1 mL/min): Mn = 44.2 kDa, Mw = 51.8 kDa, PDI = 1.2.

CdSe Quantum Dots [60]**.** Selenium precursor was prepared by mixing Se powder (0.518 g, 6.56 mmol) and tributylphosphine (1.62 g, 8.01 mmol) in a scintillation vial for 30 min. In a 50 mL three-neck round bottom flask, CdO (0.042g, 0.33 mmol), stearic acid (0.386 g, 1,36 mmol) hexadecylamine (3.88 g, 16.07 mmol), and trioctylphosphine oxide (3.88 g, 10.04 mmol) were mixed and heated with stirring up to 150 °C under flowing nitrogen until the initial reddish-brown solution became optically clear. Next, the reaction solution was heated to 320 °C, and selenium precursor was quickly injected into the reaction flask. Upon injection, the solution temperature dropped to 290 °C. After 2 min, the reaction flask was cooled down to room temperature by removing the heating mental. CdSe quantum dots were recovered by precipitation with acetone, and then washed three times with hexane/acetone mixture. The final product (yellowish powder) was vacuum dried overnight and re-dispersed in hexane.

PDTC Ligand. A 50 mL round bottom flask was charged with concentrated ammonium hydroxide (30mL, 0.435 mol) and a stir bar under flowing nitrogen. Carbon disulfide (5 mL, 0.055 mol) was then added dropwise by syringe. Next, 10 mL ethanol was added into the reaction flask. The solution was then immersed in an ice bath and aniline (5 mL, 0.083 mol) was added dropwise over 5 min. After 45 min, the reaction mixture was warmed back to room temperature. The solvent was vacuum dried, and the remaining solid was washed with chloroform. The final yellow/white powder was vacuumed dried and stored in the refrigerator (85 % yield). ^{1}H NMR (300.13 MHz, CDCl$_3$): δ (ppm) = 7.49-7.32 (Ph-*H'*s), 7.29-7.26 (-N*H*-).

CdSe Quantum Dots Ligand Exchange. 52 mg CdSe quantum dots, 4 mL dichloromethane and a few drops of hexane were added to a 20 mL scintillation vial. After completely dissolving, the solution was injected into another 20 mL vial containing PDTC ligand (4.59 g, 2.68 mmol). The mixture was then stirred at room temperature for 82 h in the dark. After the reaction, CdSe quantum dots were recovered by precipitation into methanol, and then washed three times with hexanes, followed by centrifugation. The final light yellow powder was vacuum dried and stored in the glovebox (33% yield).

Iron Oxide Nanoparticles [61]**.** Iron (III) acetylacetonate (161.5 mg, 0.46 mmol) was dispersed in a mixture of oleylamine (3.2 mL), oleic acid (2.65 mL) and 1-octadecene (12 mL) in a 50 mL three-neck round bottom flask. The mixture was heated to 110 °C and kept under vacuum for 1 h to remove moisture and oxygen within the flask. Subsequently the solution was heated to 295 °C and kept for 1 h. Afterwards, the heating mantle was removed and the solution was cooled down to room temperature. A mixture of hexane, methanol and isopropanol was used to precipitate the nanoparticle. The resulting black powder was then washed with methanol three times, dried under vacuum and re-dispersed in hexane.

Characterizations

^{1}H NMR spectra were collected on a Bruker Avance III 300 MHz spectrometer (Billerica, MA, USA) at room temperature, and referenced internally to the solvent signal. Polymer molecular weight and polydispersity index (PDI) were measured by size exclusion chromatography (SEC) using a Waters 1515 system (Milford, MA, USA) equipped with a 2414 refractive index detector and a 2707 auto-sampler. Polystyrene standards (Varian) were used for calibration, chloroform with 0.5 wt% triethylamine was used as the eluent at a flow rate of 1 mL/min. UV-visible absorption spectra were recorded on a Shimadzu UV-2401 PX spectrometer (Kyoto, Japan). Transmission

electron microscopy (TEM) images were collected with a JEOL 2010 microscope (Peabody, MA, USA), using an accelerating voltage of 200 kV.

Solar cell fabrication and testing

Indium-tin-oxide (ITO) coated glass substrates (China Shenzhen Southern Glass Display Ltd., 8 ohms/sq) were cleaned sequentially in detergent, DI water, acetone, isopropyl alcohol (15 min each), and then treated by UV Ozone (Novascan PSD series) for 45 min. Subsequently, MoO_3 (10 nm) was then deposited onto the ITO surface using an Angstrom Engineering Amond deposition system with a vacuum level $< 7 \square 10^{-8}$ Torr. Blend solutions were prepared by stirring predetermined weight ratios of polymers, nanoparticles, and PCBM in chlorobenzene at 100 °C for 10 h in a nitrogen glovebox. The active layers were casted from these blend solutions onto the MoO_3 layer by spin coating at 500 rpm for 30 s. After that, 100 nm Al electrode was thermally evaporated through patterned shadow masks.

Current-voltage (J-V) characteristics of solar cells were measured by a Keithley 2400 source meter under simulated AM 1.5 G irradiation (100 mW/cm^{-2}) provided by a Xe arc-lamp based Newport 67005 150-W solar simulator system (Franklin, MA, USA) equipped with an AM 1.5 filter, the light intensity was calibrated by a Newport thermopile detector (model 818-010-12) equipped with a Newport 1916-C Optical Power Meter.

DISCUSSION:
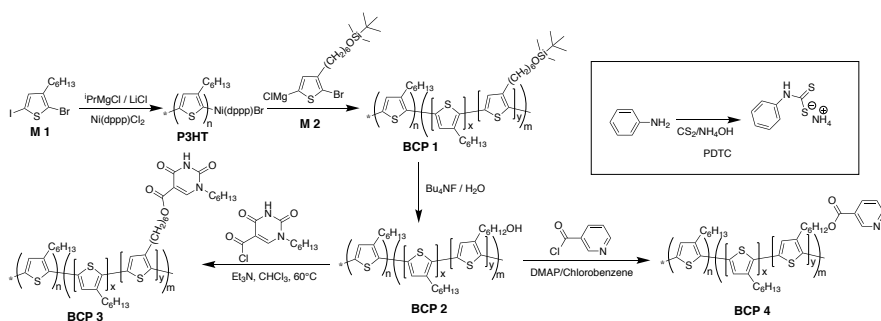
Scheme 1. Synthesis scheme of block copolymers and nanoparticle capping ligands.

The basic outline for the syntheses of two new BCPs having functionalize block carrying isoorotic acid (BCP3) or pyridine (BCP4) moieties by Grignard metathesis polymerization [62-64] is shown in Scheme 1. The as-prepared BCPs were then characterized using SEC and NMR spectroscopy. Number average molecular weights (Mn) of BCP3 and BCP4 are 27.2 kDa (PDI=1.6) and 44.2 kDa (PDI=1.2), respectively. The functional group concentration and block length ratio (n/m) are calculated to be 7%, 6:1 for BCP3, and 6%, 4.5/1 for BCP4. Non-functionalized P3HT was also prepared with good control of molecular weight and polydispersity (Mn = 19.5 kDa, PDI=1.2).
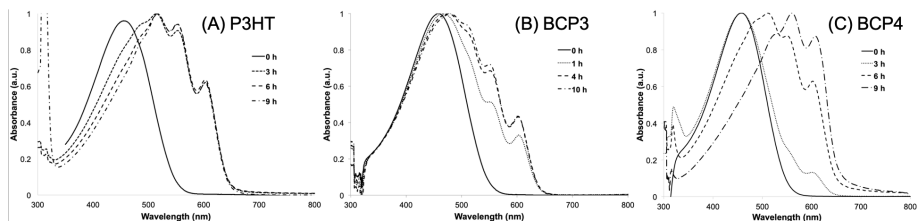
Figure 1. Time evolution of UV-vis absorption spectra of (A)P3HT, (B) BCP3 and (C) BCP4 in chlorobenzene/acetone mixed solution (4:1, v./v.).
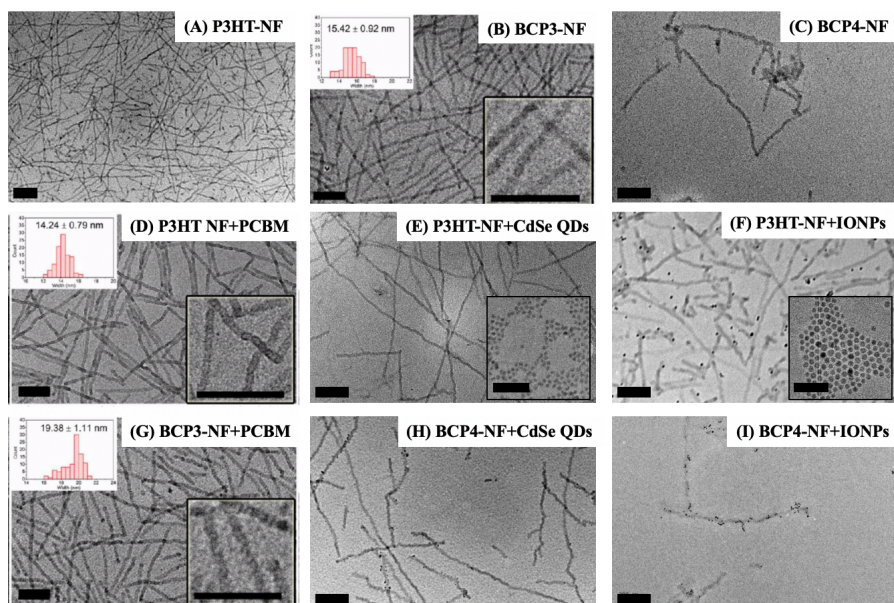

Figure 2. Transmission electron microscopy (TEM) images of (A) P3HF nanofibers (NFs); (B) BCP3 NFs; (C) BCP4 NFs; (D) P3HT NFs with the addition of PCBM; (E) P3HT NFs with the addition of CdSe quantum dos (QDs); (F) P3HT NFs with the addition of iron oxide nanoparticles (IONPs); (G) BCP3 NFs with the addition of PCBM; (H) BCP4 NFs with the addition of CdSe QDs; and (I) BCP4 NFs with the addition of IONPs (Scale bars: 200 nm). Bottom right inserts in (E) and (F) are TEM images of CdSe QDs having PDTC ligands (E) and IONPs having oleic acid ligands (F) (Scale bars: 50 nm).

NFs were then produced by following a mixed-solvent approach [65,66]. Polymers were first dissolved in chlorobenzene (5 mg/mL) followed by the addition of acetone with 4/1 (v./v.) chlorobenzene/acetone ratio. As chlorobenzene is a good solvent for both P3HT and functionalized blocks while acetone is a good solvent for the functionalized block only, the addition of acetone is expected to induce the aggregation and self-assembly of

the P3HT block into NFs. UV-Vis absorption spectroscopy was used to monitor the polymer crystallization processes for the formation of NFs, as shown in Figure 1. The red-shift and increased vibronic features observed around 500-600 nm in the absorption spectra indicated a gradual transformation of the polymer solution from the well-dissolved state to the crystalline state [67,68]. As can be seen from Figure 1, the formation of three vibronic peaks became apparent after 9 h of stirring, thus an aging time of 9 h was selected for this study. Figure 2 (A)-(C) are the TEM images of as-formed polymer NFs, which are uniform in shape. The widths of NFs were measured to be 14.28 ± 0.87 for P3HT, 15.42 ± 0.92 for BCP3, and 15.16 ± 1.66 for BCP4.

CdSe QDs [60] and IONPs [61] were synthesized based on previously reported hot injection methods using non-polar surfactants trioctylphosphine oxide (TOPO) and oleic acid (OA). The surface TOPO ligands of CdSe QDs were then replaced with shorter phenyldithiocarbamate (PDTC) ligands to facilitate charge transfer with polymer backbones and to strengthen hydrogen bonding with pyridine functional groups in the BCP4 side chains. TEM images of PDTC capped CdSe QDs and OA capped IONPs are shown in the insets of Figure 2 (E) and (F) with an average particle size of 3.37 ± 0.29 and 5.74 ± 0.72, respectively.

Polymer/NP composite NFs were then prepared by adding PCBM, CdSe or iron oxide nanoparticles (50% by weight) to the pre-formed polymer NF solutions. Morphology of the as-formed polymer composites were characterized by TEM (Figure 2 (E)-(I)). PCBM NPs were mixed with BCP1 NFs as the isoorotic acid functionalized block was specifically designed to form hydrogen bonding and π-π interactions with PCBM. On the other hand, CdSe QDs and IONPs were added into BCP4 NF solutions because pyridine has been shown to form metal-ligand coordination bonds with inorganic nanoparticles and to quench the fluorescence of QDs [69]. Also, PDTC and OA capping ligands of nanoparticles could form additional hydrogen bonds with pyridine functional groups. P3HT/nanoparticle NFs were also prepared as comparison samples because there are no specific interactions between them. As can be seen from Figure 2 (D) and (G), the widths of P3HT/PCBM NFs are similar to the widths of pure P3HT NFs, while a clear width increase was observed for BCP3/PCBM NFs, which can be explained by the attachment of PCBM particles to BCP3 NFs through non-covalent interactions with the isoorotic acid functional group. In the case of nanoparticle attachment, nanoparticles seem to be randomly distributed around P3HT NFs (Figure 2 (E)-(F)), but closely attached to both sides of BCP4 NFs (Figure 2 (H)-(I)). Again, the formation of such ordered core/shell polymer/nanoparticle NFs can be reasonably explained by the non-covalent interactions between pyridine functional groups of BCP4 and capping ligands of nanoparticles.

OPV devices were then fabricated with the device architecture of ITO glass/ MoO$_3$ (10 nm)/Active layer (100 nm)/Al (100 nm). The BHJ active layer were prepared by spin-coating of polymer/nanopartilce NF solutions with 10 mg/mL polymer concentration. Desired amounts of PCBM were also added into polymer/CdSe or iron oxide blends to improve the device charge transfer. A 150 °C post-spin coating thermal annealing was carried out for 10 min in the nitrogen filled glovebox for all devices. The device performances are summarized in Table 1.

Table 1. BHJ solar cell device performance of different polymer/NP NF mixtures.

Blends (weight ratio)	PCE[a] (%)	Jsc[b] (mA cm^{-2})	Voc[c] (V)	FF[d]
P3HT NF/PCBM (1:1)	3.32±0.21	9.93±0.53	0.57±0.01	0.59±0.01
BCP3 NF/PCBM (1:1)	4.17±0.15	11.23±0.53	0.62±0.00	0.60±0.01
BCP4 NF/CdSe QDs/PCBM (1:1:1)	0.42±0.06	3.26±1.15	0.34±0.04	0.41±0.14
BCP4 NF/IONPs/PCBM (1:0.1:1)	0.65±0.10	3.73±0.60	0.56±0.02	0.31±0.01

[a]Power conversion efficiency under simulated 100 mW/cm^2 white light irradiation. [b]Short circuit current. [c]Open circuit voltage. [d]Fill factor.

Comparing to P3HT/PCBM composite NFs, device efficiency enhancement was observed for BCP3/PCBM composite NFs, as well as higher Jsc and Voc. This performance improvement was attributed to the achievement of controlled dispersion of donor and acceptor domains in the active layer via non-covalent interactions, which resulted in enhanced charge carrier generation and improved charge transport. However, addition of CdSe QDs or IONPs yielded a low device efficiency compared to pure P3HT/PCBM blends. It has been recently reported that PDTC ligands could create traps to captures light generated holes at the surface of CdSe QDs, which led to energy loss and device degradation [70]. On the other hand, long-chain hydrocarbon-based ligands such as oleic acid have long been considered as insulating barriers around nanoparticles that could block charge transport [71]. Therefore, further investigations of finding the optimized ligands for nanoparticles which could promote change transfer are necessary to truly understand the effects of NF morphology on device performances.

CONCLUSIONS

In conclusion, we have developed a simple and efficient methodology to precisely organize nanoparticles into CP nanostructures through cooperation of several non-covalent interactions. We have designed and synthesized two new BCPs with P3HT as the backbone, and isoorotic acid or pyridine moieties in the functionalized side chains. Ligands modified nanoparticles which are designed to interact with those polar functional groups can then be attached to BCP NFs through self-assembly in mixed solvents. In addition, the resulting well-defined core/shell composite NFs have been successfully applied in BHJ solar cells. Our demonstration of employing non-covalent interactions to promote self-assembly of two incompatible components may provide new insights into the design of multifunctional superstructures.

ACKNOWLEDGMENTS

REFERENCES

1. G. Horowitz, *Adv. Mater.* **10**, 365 (1998).
2. A. Facchetti, *Mater. Today* **10**, 28 (2007).
3. C. Wang, H. Dong, W. Hu, Y. Liu and D. Zhu, *Chem. Rev.* **112**, 2208 (2012).
4. B. C. Thompson and J. M. Fréchet, *Angew. Chem.* **47**, 58 (2008).
5. G. Dennler, M. C. Scharber and C. J. Brabec, *Adv. Mater.* **21**, 1323 (2009).
6. Y.-J. Cheng, S.-H. Yang and C.-S. Hsu, *Chem. Rev.* **109**, 5868 (2009).
7. J. Chen and Y. Cao, *Acc. Chem. Res* **42**, 1709 (2009).
8. C. J. Brabec, S. Gowrisanker, J. J. Halls, D. Laird, S. Jia and S. P. Williams, *Adv. Mater.* **22**, 3839 (2010).
9. M. S. AlSalhi, J. Alam, L. A. Dass and M. Raja, *Int. J. Mol. Sci.* **12**, 2036 (2011).
10. R. Friend, R. Gymer, A. Holmes, J. Burroughes, R. Marks, C. Taliani, D. Bradley, D. Dos Santos, J. Bredas and M. Lögdlund, *Nature* **397**, 121 (1999).
11. T. D. Nielsen, C. Cruickshank, S. Foged, J. Thorsen and F. C. Krebs, *Sol. Energy Mater. Sol. Cells* **94**, 1553 (2010).
12. M. Jørgensen, J. E. Carlé, R. R. Søndergaard, M. Lauritzen, N. A. Dagnæs-Hansen, S. L. Byskov, T. R. Andersen, T. T. Larsen-Olsen, A. P. Böttiger and B. Andreasen, *Sol. Energy Mater. Sol. Cells* **119**, 84 (2013).
13. C. W. Tang, *Appl. Phys. Lett.* **48**, 183 (1986).
14. J. Halls, C. Walsh, N. C. Greenham, E. Marseglia, R. H. Friend, S. Moratti and A. Holmes, *Nature* **376**, 498 (1995).
15. G. Yu and A. J. Heeger, *J. Appl. Phys.* **78**, 4510 (1995).
16. A. Facchetti, *Mater. Today* **16**, 123 (2013).
17. G. Yu, J. Gao, J. C. Hummelen, F. Wudl and A. J. Heeger, *Science* **270**, 1789 (1995).
18. J. E. Anthony, A. Facchetti, M. Heeney, S. R. Marder and X. Zhan, *Adv. Mater.* **22**, 3876 (2010).
19. W. U. Huynh, J. J. Dittmer and A. P. Alivisatos, *Science* **295**, 2425 (2002).
20. B. Sun, E. Marx and N. C. Greenham, *Nano Lett.* **3**, 961 (2003).
21. W. J. Beek, M. M. Wienk, M. Kemerink, X. Yang and R. A. Janssen, *J. Phys. Chem. B* **109**, 9505 (2005).
22. S.-S. Li and C.-W. Chen, *J. Mater. Chem. A* **1**, 10574 (2013).
23. J. J. Halls, K. Pichler, R. H. Friend, S. Moratti and A. Holmes, *Appl. Phys. Lett.* **68**, 3120 (1996).
24. Y. Huang, E. J. Kramer, A. J. Heeger and G. C. Bazan, *Chem. Rev.* **114**, 7006 (2014).
25. C. J. Brabec, M. Heeney, I. McCulloch and J. Nelson, *Chem. Soc. Rev.* **40**, 1185 (2011).
26. X. Yang, J. Loos, S. C. Veenstra, W. J. Verhees, M. M. Wienk, J. M. Kroon, M. A. Michels and R. A. Janssen, *Nano Lett.* **5**, 579 (2005).
27. H. Tang, G. Lu, L. Li, J. Li, Y. Wang and X. Yang, *J. Mater. Chem.* **20**, 683 (2010).
28. J. Peet, J. Y. Kim, N. E. Coates, W. L. Ma, D. Moses, A. J. Heeger and G. C. Bazan, *Nat. Mater.* **6**, 497 (2007).
29. S. Samitsu, T. Shimomura, S. Heike, T. Hashizume and K. Ito, *Macromolecules* **43**, 7891 (2010).
30. E. T. Niles, J. D. Roehling, H. Yamagata, A. J. Wise, F. C. Spano, A. J. Moulé and J. K. Grey, *J. Phys. Chem. Lett.* **3**, 259 (2012).
31. K. J. Ihn, J. Moulton and P. Smith, *J. Polym. Sci.* **31**, 735 (1993).
32. N. Kiriy, E. Jähne, H.-J. Adler, M. Schneider, A. Kiriy, G. Gorodyska, S. Minko, D. Jehnichen, P. Simon and A. A. Fokin, *Nano Lett.* **3**, 707 (2003).
33. S. Samitsu, T. Shimomura, S. Heike, T. Hashizume and K. Ito, *Macromolecules* **41**, 8000 (2008).
34. J. D. Roehling, I. Arslan and A. J. Moulé, *J. Mater. Chem.* **22**, 2498 (2012).

35. W. Xu, L. Li, H. Tang, H. Li, X. Zhao and X. Yang, *J. Phys. Chem. B* **115**, 6412 (2011).
36. S. Berson, R. De Bettignies, S. Bailly and S. Guillerez, *Adv. Funct. Mater.* **17**, 1377 (2007).
37. H. Xin, F. S. Kim and S. A. Jenekhe, *J. Am. Chem. Soc.* **130**, 5424 (2008).
38. J. S. Kim, J. H. Lee, J. H. Park, C. Shim, M. Sim and K. Cho, *Adv. Funct. Mater.* **21**, 480 (2011).
39. J.-H. Kim, M. Kim, H. Jinnai, T. J. Shin, H. Kim, J. H. Park, S. B. Jo and K. Cho, *ACS Appl. Mater. Interfaces* **6**, 5640 (2014).
40. M. Sommer, S. Huettner and M. Thelakkat, *J. Mater. Chem.* **20**, 10788 (2010).
41. S. Miyanishi, Y. Zhang, K. Tajima and K. Hashimoto, *ChemComm* **46**, 6723 (2010).
42. P. D. Topham, A. J. Parnell and R. C. Hiorns, *J. Polym. Sci.* **49**, 1131 (2011).
43. I. Botiz, R. D. Schaller, R. Verduzco and S. B. Darling, *J. Phys. Chem. C* **115**, 9260 (2011).
44. R. Verduzco, I. Botiz, D. L. Pickel, S. M. Kilbey, K. Hong, E. Dimasi and S. B. Darling, *Macromolecules* **44**, 530 (2011).
45. A. M. Ramos, M. T. Rispens, J. K. van Duren, J. C. Hummelen and R. A. Janssen, *J. Am. Chem. Soc.* **123**, 6714 (2001).
46. F. Zhang, M. Svensson, M. R. Andersson, M. Maggini, S. Bucella, E. Menna and O. Inganäs, *Adv. Mater.* **13**, 1871 (2001).
47. Z. a. Tan, J. Hou, Y. He, E. Zhou, C. Yang and Y. Li, *Macromolecules* **40**, 1868 (2007).
48. M. Li, P. Xu, J. Yang and S. Yang, *J. Mater. Chem.* **20**, 3953 (2010).
49. Y. C. Lai, K. Ohshimizu, A. Takahashi, J. C. Hsu, T. Higashihara, M. Ueda and W. C. Chen, *J. Polym. Sci.* **49**, 2577 (2011).
50. L. Chen, S. Peng and Y. Chen, *ACS Appl. Mater. Interfaces* **6**, 8115 (2014).
51. K. Yao, L. Chen, F. Li, P. Wang and Y. Chen, *J. Phys. Chem. C* **116**, 714 (2012).
52. Y. Lin, J. A. Lim, Q. Wei, S. C. Mannsfeld, A. L. Briseno and J. J. Watkins, *Chem. Mater.* **24**, 622 (2012).
53. W.-C. Yen, Y.-H. Lee, J.-F. Lin, C.-A. Dai, U.-S. Jeng and W.-F. Su, *Langmuir* **27**, 109 (2011).
54. K. Palaniappan, N. Hundt, P. Sista, H. Nguyen, J. Hao, M. P. Bhatt, Y. Y. Han, E. A. Schmiedel, E. E. Sheina and M. C. Biewer, *J. Polym. Sci.* **49**, 1802 (2011).
55. F. Li, Y. Shi, K. Yuan and Y. Chen, *New J. Chem.* **37**, 195 (2013).
56. F. Li, J. Yang and Y. Qin, *J. Polym. Sci.* **51**, 3339 (2013).
57. F. Li, K. G. Yager, N. M. Dawson, J. Yang, K. J. Malloy and Y. Qin, *Macromolecules* **46**, 9021 (2013).
58. F. Li, K. G. Yager, N. M. Dawson, Y.-B. Jiang, K. J. Malloy and Y. Qin, *Chem. Mater.* **26**, 3747 (2014).
59. B. W. Watson, L. Meng, C. Fetrow and Y. Qin, *Polymers* **8**, 408 (2016).
60. R. C. Shallcross, G. S. Chawla, F. S. Marikkar, S. Tolbert, J. Pyun and N. R. Armstrong, *ACS Nano* **3**, 3629 (2009).
61. Z. Xu, C. Shen, Y. Hou, H. Gao and S. Sun, *Chem. Mater.* **21**, 1778 (2009).
62. E. E. Sheina, J. Liu, M. C. Iovu, D. W. Laird and R. D. McCullough, *Macromolecules* **37**, 3526 (2004).
63. M. C. Iovu, E. E. Sheina, R. R. Gil and R. D. McCullough, *Macromolecules* **38**, 8649 (2005).
64. T. Yokozawa and A. Yokoyama, *Chem. Rev.* **109**, 5595 (2009).
65. L. Li, G. Lu and X. Yang, *J. Mater. Chem.* **18**, 1984 (2008).
66. S. Sun, T. Salim, L. H. Wong, Y. L. Foo, F. Boey and Y. M. Lam, *J. Mater. Chem.* **21**, 377 (2011).
67. F. C. Spano, *Chem. Phys.* **325**, 22 (2006).
68. F. C. Spano, *Acc. Chem. Res* **43**, 429 (2010).
69. E. Zen'kevich, E. Sagun, A. Yarovoi, A. Shul'ga, V. Knyukshto, A. Stupak and C. Von Borczyskowski, *Opt. Spectrosc.* **103**, 958 (2007).
70. R. D. Harris, S. Bettis Homan, M. Kodaimati, C. He, A. B. Nepomnyashchii, N. K. Swenson, S. Lian, R. Calzada and E. A. Weiss, *Chem. Rev.* **116**, 12865 (2016).
71. M. A. Boles, D. Ling, T. Hyeon and D. V. Talapin, *Nat. Mater.* **15**, 141 (2016).